GENETICS AND GENOMICS

Detection of differentially expressed genes in broiler pectoralis major muscle affected by White Striping – Wooden Breast myopathies

Paolo Zambonelli,[*] Martina Zappaterra,[*] Francesca Soglia,[†] Massimiliano Petracci,[†] Federico Sirri,[†] Claudio Cavani,[†] and Roberta Davoli[*,1]

[*]*Department of Agricultural and Food Sciences (DISTAL), Bologna University, Viale G. Fanin 46, 40127 Bologna, Italy; and* [†]*Department of Agricultural and Food Sciences (DISTAL), Bologna University, Piazza Goidanich 60, 47521 Cesena, Italy*

ABSTRACT White Striping and Wooden Breast (WS/WB) are abnormalities increasingly occurring in the fillets of high breast yield and growth rate chicken hybrids. These defects lead to consistent economic losses for poultry meat industry, as affected broiler fillets present an impaired visual appearance that negatively affects consumers' acceptability. Previous studies have highlighted in affected fillets a severely damaged muscle, showing profound inflammation, fibrosis, and lipidosis. The present study investigated the differentially expressed genes and pathways linked to the compositional changes observed in WS/WB breast muscles, in order to outline a more complete framework of the gene networks related to the occurrence of this complex pathological picture. The biochemical composition was performed on 20 pectoralis major samples obtained from high breast yield and growth rate broilers (10 affected vs. 10 normal) and 12 out of the 20 samples were used for the microarray gene expression profiling (6 affected vs. 6 normal). The obtained results indicate strong changes in muscle mineral composition, coupled to an increased deposition of fat. In addition, 204 differentially expressed genes (DEG) were found: 102 up-regulated and 102 down-regulated in affected breasts. The gene expression pathways found more altered in WS/WB muscles are those related to muscle development, polysaccharide metabolic processes, proteoglycans synthesis, inflammation, and calcium signaling pathway. On the whole, the findings suggest that a multifactorial and complex etiology is associated with the occurrence of WS/WB muscle abnormalities, contributing to further defining the transcription patterns associated with these myopathies.

Key words: chicken, pectoralis major, wooden breast, white striping, microarray

2017 Poultry Science 95:2771–2785
http://dx.doi.org/10.3382/ps/pew268

INTRODUCTION

In the past few decades, genetic selection for high breast yield and growth rate hybrids led to a dramatic increase in the incidence of several muscle myopathies and abnormalities (Dransfield and Sosnicki, 1999; Sandercock et al., 2009; Petracci and Cavani, 2012). Recently, it was found that up to 40% of broiler hybrids raised under commercial conditions were affected by white-striping (**WS**) with in some of those cases also the contextual occurrence of wooden breast (**WB**) (Lorenzi et al., 2014). As a consequence of the impaired visual appearance and consumers' acceptability, fillets with severe WS and WB are downgraded, leading to considerable economic losses for poultry meat industry (Kuttappan et al., 2012; Petracci et al., 2015). Furthermore, these myopathies exert a detrimental effect on quality traits and, as a result of the altered composition and reduced protein functionality (i.e., ability to hold/bind water, gel formation), may negatively affect both nutritional value and technological traits of meat (Mudalal et al., 2014, 2015). The emerging issue of WS/WB chicken fillets has to date no solution, as, despite the increasing number of studies aimed at investigating this defect, knowledge concerning WS/WB occurrence is still incomplete and no certainty has been reached about the causes of this myopathy. Nevertheless, WS incidence is probably related to the animal genetics as its occurrence showed a heritability ranging from 0.338 (Bailey et al., 2015) to 0.65 (Alnahhas et al., 2016) depending on the studies.

The studies that have already been assessed on WS- and WB-affected breast muscles of high breast yield broilers identified through the biochemical and histological analysis an acutely inflamed and damaged muscle, with the presence of lipidosis and fibrosis (Mazzoni et al., 2015; Soglia et al., 2016).

Received March 24, 2016.
Accepted June 16, 2016.
[1]Corresponding author: roberta.davoli@unibo.it

Considering this scenario, the present study was aimed to compare the genomic transcription profile of WS/WB abnormal (**ABN**) pectoralis major muscles respect to the normal ones (**NORM**) and obtain additional information about the gene networks, possibly leading to the phenotypes typically related to WS/WB abnormalities.

MATERIALS AND METHODS

Sample Selection and Preparation

Twenty boneless and skinless pectoralis major muscles were selected from the same flock of Ross 708 broilers (males, weighing around 3.7 kg) in the deboning area of a commercial processing plant within 2 h post-mortem. Birds belonging to this flock were farmed and slaughtered under commercial conditions according to Italian and European law for broiler chicken production. At slaughterhouse, the birds were electrically stunned in agreement with the Council Regulation (EC) No. 1099/2009 on the protection of animals at the time of killing. All slaughter procedures were monitored by the veterinary team appointed by the Italian Ministry of Health. Fillets were selected, evaluated for the presence/absence of muscle abnormalities, and classified as NORM and ABN according to the criteria proposed by Kuttappan et al. (2012) and Sihvo et al. (2014). In particular, 10 NORM fillets without any hardened area and white striations and 10 ABN samples exhibiting diffused, hardened areas and pale-bulging caudal end coupled with superficial white striations in the cranial part were packaged and transported to the laboratory under refrigerated conditions (0 to 2°C). At the slaughterhouse, for the gene expression analysis, pieces of the 12 fillets showing the most extreme WS/WB phenotype among the 20 samples were chosen (6 NORM and 6 ABN), immediately frozen in liquid nitrogen, then stored at –80°C until RNA extraction. RNA was extracted using TRIZOL reagent (Invitrogen Corporation, Carlsbad, CA), as described in Davoli et al. (2011).

Quality and Technological Traits

At 24 h post-mortem, fillets were individually weighted and color was measured in triplicate on the ventral surface using a Chroma Meter CR-400 (Minolta Corp., Milan, Italy). Furthermore, the morphometric measurements (length, width, and height, expressed in mm) were assessed with an electronic caliper as previously described by Mudalal et al. (2015) and ultimate pH evaluated according to the procedure described by Jeacocke (1977). Then, a parallelepiped sample (8 × 4 × 3 cm weighing approximately 80 g) was cut from the cranial part of each fillet and used to assess drip loss (percentage of weight lost as a consequence of refrigerated storage), cooking loss (after 45 min heating treatment at 80°C in a water bath), and Allo-Kramer shear force by using the procedures described in Petracci et al. (2013). Another sample (8 × 4 × 2 cm, weighing approximately 60 g) was excised from the middle section of the fillet, labeled and tumbled with 20% (wt/wt) sodium chloride (6%) and sodium tripolyphosphate (1.8%) marinade solution. Then, marinade uptake, cooking loss (after 25 min heating treatment at 80°C in a water bath), processing yield, and Allo-Kramer shear force were assessed (Petracci et al., 2013).

Composition of Breast Fillets

Proximate (moisture, protein, fat, ash and collagen) and mineral composition of ABN and NORM fillets was determined on each pectoralis major muscle applying standard methods. In particular, moisture and ash contents were calculated as the percentage of weight lost after drying 5 g of sample in oven (105°C for 16 h) and incineration in muffle furnace (at 525°C), respectively (AOAC, 1990). Crude proteins were determined according to Kjeldahl method by using copper sulphate as catalyst whereas total lipid amount was estimated by diethyl ether extraction performed with Soxhlet apparatus (AOAC, 1990). In addition, the colorimetric method proposed by Kolar (1990) was applied in order to determine hydroxyproline content and calculate the total amount of collagen (considering 7.5 as conversion factor). Inductively Coupled Plasma-Optic Emission Spectrometry technique (ICP-OES) was used in order to quantify minerals (Mg, K, P, Na, and Ca) following the procedure suggested by the Environmental Protection Agency (EPA, 1996; 2007). Blanks were run to check for chemicals purity and reference materials (CRM GBW 09101, human hair control, Shanghai Institute of Nuclear Research Academia Sinica; CRM 201505 and 201605 Trace Element Whole Blood, Seronorm, Billingsad, Norway) were used to verify the accuracy. Finally, minerals content in tissues was calculated and expressed as mg 100 g^{-1} breast muscle.

SDS-PAGE Analysis of Muscle Proteins

One-dimensional SDS-PAGE analysis was carried out in order to evaluate the myofibrillar and sarcoplasmic proteins profile of ABN and NORM fillets following the procedure described by Liu et al. (2014) and removing the interfering substances such as salts, detergents, denaturants or organic solvents by READYPREP 2-D cleanup kit (Bio-Rad Laboratories, Hercules, CA). Before loading, protein concentration was determined according to the Bradford assay (Bradford, 1976) and runs performed following the procedure described by Soglia et al. (2016). A molecular weight marker (Precision plus Standard protein, all blue pre-stained, Bio-Rad) was loaded on the first well of each gel and used to calculate the molecular weight of the separated bands. Each band was identified based on purified sarcoplasmic and myofibrillar proteins identified by

mass spectrometry from literature (Zapata et al., 2012; Li et al., 2015) and the concentration expressed as relative abundance (%).

Statistical Analysis of Meat Quality Evaluation

Differences on meat quality and technological traits, composition as well as myofibrillar and sarcoplasmic protein profiles for ABN and NORM samples, were tested by 2-tailed Student's t test. Statistical analyses were performed with SAS version 9.4 (SAS 9.4, Cary, NC. SAS Institute Inc.) and the nominal P-value ≤ 0.05 was considered as significance threshold.

Microarray Expression Profiling

Each extracted RNA was checked for integrity and quality using an Agilent BioAnalyzer 2100, retrotranscribed, amplified, labeled and applied to Affymetrix GeneChip Chicken Gene 1.1 ST v1 expression array by an outsource company (Cogentech Microarray Unit, Milan, Italy). All analytic procedures performed on microarray data were carried out using Partek Genomics Suite software, version 6.6 Copyright 2014 (Partek Inc., St. Louis, MO). Gene expression profiles from the 6 ABN biological replicates were compared to the 6 NORM biological ones in order to identify differentially expressed genes (**DEGs**) indicated with the genes fold change (**FC**) values between ABN an NORM broiler. FC filtering criteria combined with statistical t-test with FDR applied for multiple testing corrections were used to identify DEGs between the 2 conditions. The expression data obtained have been submitted to U.S. National Center for Biotechnology Information GEO database with the accession number GSE79276.

Validation by Quantitative Real Time-PCR

The results of the array expression analysis were validated by quantitative real-time PCR (**qPCR**). After DNAse treatment (TURBO DNA-freeTM, Ambion, Applied Biosystems), 1 μg of total RNA was reverse transcribed using the iScript cDNA Synthesis kit (Bio-Rad) according to the manufacturers' instructions. QPCR was performed on Rotor Gene^{TM} 6000 (Corbett Life Science, Concorde, New South Wales, Australia) using 5 μL of SYBR® Premix Ex Taq^{TM} (TAKARA Bio INC, Olsu, Shiga, Japan), 5 pmol of each primer, 2 μL of cDNA template diluted 1:10 and then was made up to the total volume of 10 μL with water. Rotor Gene^{TM} 6000 protocol was optimized using specific annealing temperatures for each primer couple (Supplementary Table 1). The samples were first used to assess the expression level of 3 candidate-normalizing genes: glyceraldehyde-3-phosphate dehydrogenase (***GAPDH***), ribosomal protein L32 (***RPL32***), tyrosine 3-monooxygenase/tryptophan 5-monooxygenase activation protein, zeta (***YWHAZ***). Primers and PCR conditions used are reported in Supplementary Table 1. The expression levels of these 3 genes were evaluated using NormFinder and *GAPDH* and *YWHAZ*, the 2 most stably expressed normalizing genes, used as reference genes. For each gene selected for validating the results of the expression array, an external primer pair to obtain the amplicon for the standard curve and an internal primer pair for the qPCR (Supplementary Table 1) were designed. For the validation of the microarray results, 5 genes were chosen: crystallin alpha B (***CRYAB***), myoglobin (***MB***), glucosamine (UDP-N-acetyl)-2-epimerase/N-acetylmannosamine kinase (***GNE***), utrophin (***UTRN***), and prostaglandin F receptor (***PTGFR***).

Threshold cycles obtained for the samples were converted by Rotor Gene 6000 to mRNA molecules/μL using for each gene the relative standard curve (Pfaffl, 2004; Zambonelli et al., 2016). Moreover, the average mRNA molecules/μL for each sample was normalized dividing the gene mRNA molecules/μL by the geometric average of *GAPDH* and *YWHAZ* mRNA molecules/μL in the given sample, as described in Zambonelli et al. (2016). Differences on the expression level calculated for ABN and NORM samples were tested by 2-tailed Student's t test. Statistical analyses were performed with SAS version 9.4 (SAS 9.4, Cary, NC. SAS Institute Inc.) and the nominal P-value ≤ 0.05 was considered as significance threshold.

Furthermore, in addition to the genes found differentially expressed, also ATPase sarcoplasmic/endoplasmic reticulum Ca^{2+} transporting 2 (***ATP2A2***) gene expression was tested through qPCR, and its absolute expression normalized using *GAPDH* and *YWHAZ* as normalizing genes.

Functional Characterization

Functional annotation, classification and annotation clustering of selected gene sets were carried out by DAVID Tools 6.7 (Huang et al., 2009a,b) using Biological Processes, Molecular Function gene ontology categories and KEGG pathways. A threshold for significance of $P < 0.05$ was considered to choose the significant functional categories.

The precise identification of the regulated snoRNAs was obtained by BLAST analysis (https://blast.ncbi.nlm.nih.gov/Blast.cgi?PAGE_TYPE = BlastSearch) using blastn algorithm and standard parameters.

In order to identify the codified name and the putative target genes of the differentially expressed micro-RNAs (**miRNAs**) the miRBase website (http://www.mirbase.org/) was consulted in order to check the predicted chicken target genes resulting by the inspection of the correspondences obtained using miRDB (http://mirdb.org/miRDB/index.html) and TargetScan (http://www.targetscan.org/) databases available in miRBase.

Table 1. Effect of breast abnormalities on weight, dimension and texture of raw chicken fillets.

Trait	Breast meat category[1]		SEM	*P*-value
	NORM	ABN		
Weight (g)	218.27	301.51	11.262	<0.0001
Top height (H1)[2] (mm)	37.82	44.31	0.959	0.0001
Middle height (H2)[3] (mm)	23.43	34.52	1.478	<0.0001
Bottom height (H3)[4] (mm)	7.60	12.70	0.808	0.0003
Length (mm)	185.03	194.10	2.815	0.1088
Length (mm/g)	85.42	64.76	2.738	<0.0001
Width (mm)	73.95	77.01	1.173	<0.0001
Width (mm/g)	34.37	25.64	1.279	0.0001

[1]NORM = without any abnormalities; ABN = with both white striping and wooden breast abnormalities.
[2]H1 measured at the thickest point in the cranial part.
[3]H2 measured at half distance of the breast length.
[4]H3 measured as the vertical distance far from the end of the caudal part by 1 cm in a dorsal direction.
SEM = standard error of mean.

Table 2. Effect of breast abnormalities on quality traits of chicken meat.

Trait	Breast meat category[1]		SEM	*P*-value
	NORM	ABN		
Raw meat				
pHu	5.87	6.06	0.03	0.0039
CIE-L*	54.50	52.52	0.51	0.0486
CIE-a*	0.82	1.41	0.16	0.0568
CIE-b*	3.92	3.62	0.21	0.4800
Drip loss (%)	1.07	1.06	0.06	0.9166
Cooking loss (%)	21.45	34.04	1.73	<0.0001
Allo-Kramer shear force (kg/g)	4.26	7.54	0.68	0.0110
Marinated meat				
Uptake (%)	18.33	7.44	1.34	<0.0001
Cooking loss (%)	14.53	21.94	1.12	0.0001
Yield (%)	101.12	83.83	2.12	<0.0001
Allo-Kramer shear force (kg/g)	2.13	4.08	0.28	<0.0001

[1]NORM = without any abnormalities; ABN = with both white striping and wooden breast abnormalities.
SEM = standard error of mean.

RESULTS

Quality and Technological Traits

The effects of muscle abnormalities on fillet weight and dimensions are displayed in Table 1. Overall, ABN samples exhibited higher weight ($P < 0.001$) coupled with increased length, width, and middle height. As for raw meat quality (Table 2), ABN fillets were paler and revealed higher redness and ultimate pH values. Additionally, both raw and marinated ABN samples exhibited higher cooking losses ($P < 0.001$) and lower marinade uptake ($P < 0.001$). Besides, if compared with NORM group, a sharp increase in shear force value was measured in raw and marinated ABN fillets ($P < 0.001$).

Chemical and Mineral Composition

The occurrence of WS/WB abnormalities exerted a relevant impact on proximate and minerals compositions of the affected muscles (Table 3). In particular, ABN fillets exhibited higher ($P < 0.001$) moisture, fat and collagen contents coupled with reduced ash and proteins ($P < 0.001$) levels. As for mineral composition, no differences were found in potassium content whereas ABN samples had lower magnesium and phosphorus levels. Additionally, an increased amount of sodium ($P < 0.001$) and calcium was observed in ABN fillets.

Identification of Differentially Expressed Proteins

With regard to myofibrillar proteins pattern (Table 4), 9 bands having molecular weight from 16 to 220 kDa were identified. In detail, lower relative abundance of slow-twitch light chain myosin (**LC1**, 27.5 kDa) coupled with higher amount of 70 kDa myosin heavy chain (**MHC**) fragment were found in ABN samples.

As for sarcoplasmic protein pattern (Table 5), eleven bands, having molecular weight ranging from 25 to 114 kDa, were detected and almost all the enzymes involved in glucose metabolism differed between ABN and NORM groups. In particular, compared with normal, ABN fillets exhibited lower amount of phosphoglycerate mutase (**PGAM**, 25 kDa), creatine kinase

Table 3. Effect of breast abnormalities on chemical composition of chicken meat.

Trait	Breast meat category[1]		SEM	*P*-value
	NORM	ABN		
Moisture (%)	74.64	76.82	0.39	0.0014
Fat (%)	0.79	1.79	0.17	0.0007
Ash (%)	1.46	1.19	0.06	0.0138
Collagen (%)	1.16	1.35	0.04	0.0163
Protein (%)	23.37	18.45	0.69	<0.0001
Magnesium, Mg (mg/100 g)	35.99	32.59	0.80	0.0272
Potassium, K (mg/100 g)	359.31	362.96	6.59	0.7927
Phosphorus, P (mg/100 g)	222.63	207.30	3.70	0.0326
Sodium, Na (mg/100 g)	37.82	75.06	5.76	0.0001
Calcium, Ca (mg/100 g)	7.81	11.32	0.69	0.0059

[1]NORM = without any abnormalities; ABN = with both white striping and wooden breast abnormalities.
SEM = standard error of mean.

Table 4. Effect of breast abnormalities on myofibrillar proteins composition of chicken meat.

Protein (1)	Mol. Wt.	Breast meat category[1]		SEM	*P*-value
		NORM	ABN		
LC3	16 kDa	12.41	15.68	1.07	0.1290
LC2	19 kDa	3.58	3.50	0.40	0.9208
LC1	27.5 kDa	13.71	8.01	1.09	0.0043
30 kDa troponin T fragment	29 kDa	4.00	4.96	0.29	0.1019
troponin T	34 kDa	4.81	4.67	0.30	0.8200
actin	42 kDa	33.81	36.88	1.77	0.4062
desmin	53 kDa	5.25	6.29	0.40	0.2022
70 kDa MHC fragment.	70 kDa	4.77	6.91	0.47	0.0161
MHC	220 kDa	16.19	13.12	1.77	0.4062

[1]NORM = without any abnormalities; ABN = with both white striping and wooden breast abnormalities.
SEM = standard error of mean.
(1) MHC = Myosin heavy chain; LC = Myosin light chain.

Table 5. Effect of breast abnormalities on sarcoplasmic proteins composition of chicken meat.

Protein (1)	Mol. Wt.	Breast meat category[1]		SEM	*P*-value
		NORM	ABN		
PGAM	25 kDa	7.44	5.54	0.33	0.0010
TPIS	26.4 kDa	7.16	6.50	0.24	0.1771
CA	31.8 kDa	9.42	8.27	0.58	0.3388
LDH	34 kDa	18.76	22.85	0.85	0.0104
G3P	36 kDa	10.33	13.26	0.62	0.0116
ALDO	39 kDa	7.06	10.42	0.62	0.0025
KCRM	43 kDa	11.23	9.89	0.32	0.0327
GPI	58 kDa	8.31	4.86	0.67	0.0053
KPYM	68 kDa	6.06	4.17	0.36	0.0037
PYGL	90 kDa	13.28	15.79	0.60	0.0301
AT2A2	114 kDa	0.00	1.86	0.35	0.0029

[1]NORM = without any abnormalities; ABN = with both white striping and wooden breast abnormalities.
SEM = standard error of mean.
(1) Abbreviations obtained from www.uniprot.org: PGAM = Phophoglycerate mutase; TPIS = Triosephosphate isomerase 1; CA = carbonic anhydrase; LDH = Lactate dehydrogenase; G3P = Glyceraldehyde dehydrogenase; ALDO = Aldolase; KCRM = Creatine kinase; GPI = Phosphoglucose isomerase; KPYM = Pyruvate kinase; PYGL = Glycogen phosphorylase; AT2A2 = Calcium-Transporting ATPase Sarcoplasmic Reticulum Type Slow Twitch Skeletal Muscle Isoform.

(**KCRM**, 43 kDa), phosphoglucose isomerase (**GPI**, 58 kDa) and pyruvate kinase (**KPYM**, 68 kDa) together with higher relative abundance of lactate dehydrogenase (**LDH**, 34 kDa), glyceraldehyde dehydrogenase (**G3P**, 36 kDa), aldolase (**ALDO**, 39 kDa) and glycogen phosphorylase (**PYGL**, 90 kDa). In addition, ABN samples exhibited higher calcium-transporting ATPase sarcoplasmic reticulum type slow twitch skeletal muscle isoform (**AT2A2**, 114 kDa, coded by *ATP2A2* gene).

Profiling of Differentially Expressed Genes

Comparing the gene expression profiles obtained for ABN vs. NORM samples, 207 differentially expressed

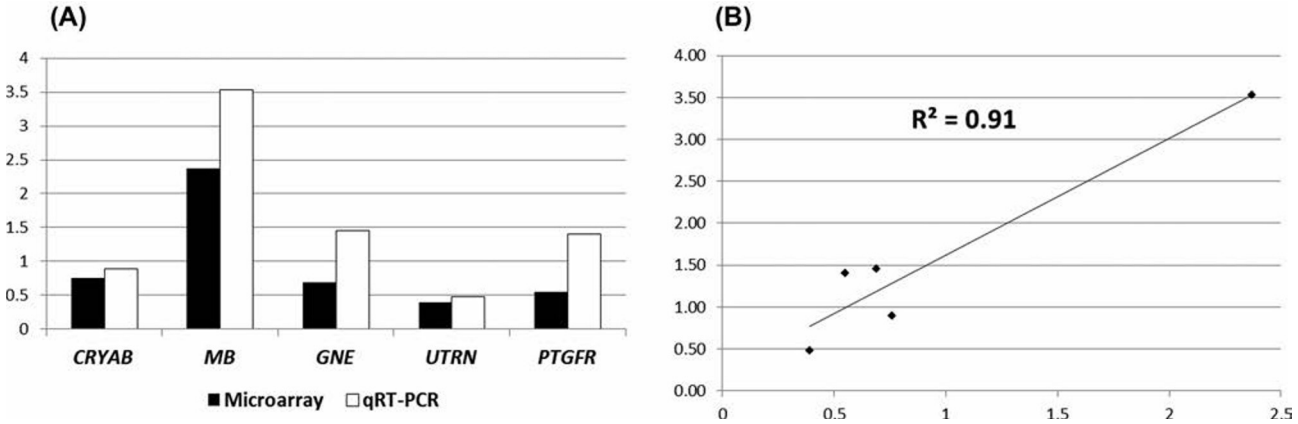

Figure 1. Validation by qPCR of 5 differentially expressed genes obtained by microarray analysis. (A) Fold changes values obtained from microarrays, (black bars) and from qPCR data (white bars), for the 5 tested genes; (B) scatterplot showing the good correlation between the fold changes values calculated with the 2 experimental methods.

genes (**DEG**) were found: 103 up-regulated and 104 down-regulated in ABN chickens (Supplementary Table 2). The overexpressed gene poly(A) binding protein, cytoplasmic 1 (***PABPC1***) (NM_001031597) was found twice on the list of DEG whereas the uncharacterized under expressed gene CD218879 was found 3 times among the probes included in the microarray then the number of unique DEG is 102 for the up-regulated and 102 also for the down-regulated. In both cases, the trend of expression was the same for the doublets or triplets of gene probe and the fold changes detected are identical or similar. Among the more expressed genes in ABN samples only 3 were currently not identified both in chickens and human genome. For the less expressed genes in ABN chickens, the situation found was more complex because we identified fifteen uncharacterized genes as described before but we found represented in this group also some short noncoding RNAs. In particular, we observed the presence of 4 small nucleolar RNAs (**snoRNAs**; GGN5, GGN50, GGN73, and GGN98) and of 5 miRNAs (MIR196B, MIR205, MIR1600, MIR1716, and MIR1805).

The differentially expressed genes mapped on all chicken chromosomes from 1 to 28 and one was mapped each on chromosome 30, mitochondrion genome (tRNA-Asn gene) and on the unassigned linkage group LGE64. Furthermore, 6 genes currently have not been located on the chicken genome sequence and 4 of them are not characterized yet. The intensity of the differential expression for the less expressed genes in ABN chickens varied between –1.07 and –2.71 FC with 5 genes showing a FC below –2. Among the overexpressed genes, the range of FCs was between 1.16 and 9.87 with 12 genes showing FC values between 2 and 3 and 3 genes showed higher values (nuclear factor, interleukin 3 regulated (***NFIL3***) 3.24, myoglobin (***MB***) 5.17, cysteine and glycine-rich protein 3 (cardiac LIM protein) (***CSRP3***) 9.87. In general, the moderate level of differences in expression can suggest the simultaneous involvement of several genes needed for the definition of the abnormal pectoralis major muscle phenotypes.

Validation by qPCR

In order to confirm the results obtained with microarray, we selected 5 genes (*CRYAB*, *MB*, *GNE*, *UTRN*, *PTGFR*) that were analyzed by qPCR and the data obtained were compared with the expression profiles obtained using microarrays (Figure 1A). The expression level of all validated genes was in agreement between the 2 analyses showing a very good correlation ($R^2 = 0.91$, Figure 1B). Moreover, we tested by qPCR also the expression level of *ATP2A2* mRNA, a gene not present among the probes of the utilized microarray as the protein coded by this gene was found differentially expressed between ABN and NORM samples using SDS-PAGE analysis (Table 2). The results of the qPCR experiment for the *ATP2A2* gene confirmed the difference of expression detected by SDS-PAGE analysis. According to this result, we also considered *ATP2A2* for the functional characterization of the differentially expressed genes.

Functional Characterization of the Differentially Expressed Coding Genes

A functional classification was carried out using DAVID tools (Table 6). The significant annotation clusters represented are related to several categories of the Biological Processes section according to the Gene Ontology classification such as developmental processes (in particular, muscle organ development), polysaccharide metabolic processes, response to reactive oxygen species and immune response, regulation of cell cycle, mRNA export from nucleus, blood vessels morphogenesis, intracellular transport, sensory perception of light stimulus. Interestingly, the unique KEGG pathway

Table 6. DAVID functional clustering obtained considering all the differentially expressed genes.

Category	Term	Count	*P*-value	Genes
Annotation Cluster 1	Enrichment Score: 1.63			
GOTERM_BP_ALL	GO:0032502~developmental process	43	2.39E-03	CHERP, PLXNA1, AGFG1, FHL1, UTRN, UGDH, ROMO1, PRRX2, MYT1, ADA, HEMGN, DFNB31, IGSF10, MUSK, BHLHA15, RASGRP1, PPL, IL1B, AP3D1, PLCD1, DOPEY2, ODF1, MB, APC, STX3, CRYAB, NEUROG1, SNAI2, DBH, CSRP3, UBP1, PPP1CB, EPHA2, SMTN, ATP2A2, GNAQ, PLN, USP22, HSPD1, GADD45B, SLITRK6, WNT7A, TMOD1
GOTERM_BP_ALL	GO:0007275~multicellular organismal development	38	8.33E-03	CHERP, PLXNA1, AGFG1, FHL1, UTRN, UGDH, PRRX2, MYT1, ADA, HEMGN, DFNB31, IGSF10, MUSK, PPL, IL1B, PLCD1, DOPEY2, ODF1, MB, APC, STX3, CRYAB, NEUROG1, SNAI2, DBH, CSRP3, UBP1, PPP1CB, EPHA2, SMTN, ATP2A2, GNAQ, PLN, HSPD1, USP22, GADD45B, SLITRK6, WNT7A
GOTERM_BP_ALL	GO:0030154~cell differentiation	24	1.65E-02	STX3, AGFG1, FHL1, UTRN, NEUROG1, MYT1, CSRP3, ADA, EPHA2, HEMGN, IGSF10, DFNB31, MUSK, GNAQ, BHLHA15, PPL, RASGRP1, ODF1, SLITRK6, GADD45B, WNT7A, TMOD1, APC, MB
GOTERM_BP_ALL	GO:0048869~cellular developmental process	24	2.55E-02	STX3, AGFG1, FHL1, UTRN, NEUROG1, MYT1, CSRP3, ADA, EPHA2, HEMGN, IGSF10, DFNB31, MUSK, GNAQ, BHLHA15, PPL, RASGRP1, ODF1, SLITRK6, GADD45B, WNT7A, TMOD1, APC, MB
GOTERM_BP_ALL	GO:0048856~anatomical structure development	32	3.22E-02	CHERP, AGFG1, FHL1, UTRN, UGDH, PRRX2, MYT1, ADA, DFNB31, IGSF10, MUSK, PPL, IL1B, PLCD1, MB, APC, STX3, CRYAB, NEUROG1, SNAI2, DBH, CSRP3, UBP1, EPHA2, SMTN, ATP2A2, GNAQ, PLN, HSPD1, SLITRK6, WNT7A, TMOD1
GOTERM_BP_ALL	GO:0032501~multicellular organismal process	48	4.83E-02	CHERP, PLXNA1, AGFG1, TACR2, FHL1, UTRN, UGDH, CNGB1, PRRX2, MYT1, ADA, KIFC3, HEMGN, DFNB31, IGSF10, MUSK, RAX2, PPL, P2RY1, IMPG2, IL1B, PLCD1, DOPEY2, ODF1, PPAP2A, PLCB2, MB, APC, STX3, CRYAB, KRT12, NEUROG1, SNAI2, DBH, CSRP3, UBP1, PPP1CB, EPHA2, SMTN, EPS8, ATP2A2, GNAQ, PLN, USP22, HSPD1, GADD45B, SLITRK6, WNT7A
Annotation Cluster 2	Enrichment Score: 1.18			
GOTERM_BP_ALL	GO:0007517~muscle organ development	7	1.12E-02	MUSK, SMTN, CRYAB, FHL1, PLN, UTRN, CSRP3
Annotation Cluster 3	Enrichment Score: 1.07			
GOTERM_BP_ALL	GO:0005976~polysaccharide metabolic process	5	1.70E-02	GBE1, GNE, UGDH, PPP1CB, CHST1
GOTERM_BP_ALL	GO:0006066~alcohol metabolic process	9	3.69E-02	GPD1L, ACAA2, GBE1, GNE, CRYAB, UGDH, DBH, PPP1CB, CHST1
GOTERM_BP_ALL	GO:0005996~monosaccharide metabolic process	6	4.74E-02	GBE1, GNE, CRYAB, UGDH, PPP1CB, CHST1
Annotation Cluster 4	Enrichment Score: 1.04			
GOTERM_BP_ALL	GO:0048514~blood vessel morphogenesis	6	3.96E-02	IL1B, PLCD1, PRRX2, DBH, CSRP3, UBP1
Annotation Cluster 5	Enrichment Score: 1.01			
GOTERM_BP_ALL	GO:0000302~response to reactive oxygen species	4	2.88E-02	CRYAB, ROMO1, ADA, MB
Annotation Cluster 6	Enrichment Score: 0.98			
GOTERM_BP_ALL	GO:0051726~regulation of cell cycle	8	2.78E-02	SKP2, IL1B, NEUROG1, USP22, OBFC2A, GADD45B, PPP1CB, APC
Annotation Cluster 7	Enrichment Score: 0.95			
KEGG_PATHWAY	hsa04020:Calcium signaling pathway	8	1.03E-03	GNAQ, ATP2A2, TACR2, PLN, HTR4, PLCD1, PTGFR, PLCB2
GOTERM_MF_ALL	GO:0004629~phospholipase C activity	3	2.89E-02	GNAQ, PLCD1, PLCB2

Table 6. – continued.

Category	Term	Count	*P*-value	Genes
Annotation Cluster 8	Enrichment Score: 0.94			
GOTERM_BP_ALL	GO:0006406~mRNA export from nucleus	3	3.44E-02	ZC3H3, AGFG1, SMG7
GOTERM_BP_ALL	GO:0006913~nucleocytoplasmic transport	5	4.99E-02	ZC3H3, AGFG1, SMG7, SPTBN1, TOB1
Annotation Cluster 9	Enrichment Score: 0.93			
GOTERM_BP_ALL	GO:0046907~intracellular transport	14	5.44E-03	ZC3H3, SYNRG, STX3, AGFG1, AP1G1, SMG7, ATP2A2, BHLHA15, RANBP3, SPTBN1, AP3D1, GOSR2, DOPEY2, TOB1
GOTERM_BP_ALL	GO:0051649~establishment of localization in cell	15	1.85E-02	ZC3H3, SYNRG, STX3, AGFG1, AP1G1, SMG7, ATP2A2, BHLHA15, RANBP3, AP3D1, SPTBN1, GOSR2, DOPEY2, WNT7A, TOB1
GOTERM_BP_ALL	GO:0051641~cellular localization	15	3.51E-02	ZC3H3, SYNRG, STX3, AGFG1, AP1G1, SMG7, ATP2A2, BHLHA15, RANBP3, AP3D1, SPTBN1, GOSR2, DOPEY2, WNT7A, TOB1
Annotation Cluster 10	Enrichment Score: 0.74			
GOTERM_BP_ALL	GO:0002824~positive regulation of adaptive immune response based on somatic recombination of immune receptors built from immunoglobulin superfamily domains	3	2.88E-02	IL1B, HSPD1, ADA
GOTERM_BP_ALL	GO:0050870~positive regulation of T cell activation	4	2.98E-02	AP3D1, IL1B, HSPD1, ADA
GOTERM_BP_ALL	GO:0002821~positive regulation of adaptive immune response	3	3.06E-02	IL1B, HSPD1, ADA
Annotation Cluster 11	Enrichment Score: 0.69			
GOTERM_BP_ALL	GO:0002026~regulation of the force of heart contraction	3	8.61E-03	ATP2A2, PLN, CSRP3
GOTERM_BP_ALL	GO:0008016~regulation of heart contraction	4	3.09E-02	ATP2A2, PLN, CSRP3, ADA
Annotation Cluster 12	Enrichment Score: 0.65			
GOTERM_BP_ALL	GO:0050953~sensory perception of light stimulus	6	4.30E-02	DFNB31, RAX2, IMPG2, KRT12, CNGB1, KIFC3
GOTERM_BP_ALL	GO:0007601~visual perception	6	4.30E-02	DFNB31, RAX2, IMPG2, KRT12, CNGB1, KIFC3
Annotation Cluster 13	Enrichment Score: 0.60			
GOTERM_BP_ALL	GO:0051726~regulation of cell cycle	8	2.78E-02	SKP2, IL1B, NEUROG1, USP22, OBFC2A, GADD45B, PPP1CB, APC
GOTERM_BP_ALL	GO:0043085~positive regulation of catalytic activity	10	4.14E-02	PSMB4, GNAQ, P2RY1, BIRC7, IL1B, HSPD1, PPAP2A, GADD45B, PPP1CB, PLCB2
Annotation Cluster 14	Enrichment Score: 0.55			
GOTERM_BP_ALL	GO:0003012~muscle system process	6	1.68E-02	SMTN, TACR2, CRYAB, UTRN, IL1B, MB

represented was the calcium signaling pathway. By analysing this regulated pathway, we observed that 5 DEG, all overexpressed, were involved in the calcium homeostasis within the cells. Furthermore, 2 down-regulated genes, 5-hydroxytryptamine (serotonin) receptor 4 (***HTR4***) and tachykinin receptor 2 (***TACR2***), were also included in the calcium signaling pathway as reported by DAVID analysis.

Functional Characterization of the Differentially Expressed Noncoding Genes

Among the less expressed genes detected in ABN samples, the presence of 9 noncoding RNAs is remarkable.

The first type of this category of genes is snoRNAs that are noncoding transcripts active within the nucleolus of the cells and that guide molecules for site specific modifications of other RNAs. By BLAST analysis (Table 7), we found that the 4 detected DE snoRNAs belong to the H/ACA box family and are involved in the pseudouridynilation of rRNAs and snoRNAs, changing an uridine to the pseudouridine isomer (Zhang et al., 2009; Holley and Topkara, 2011), which plays a key role in the activation of ribosome function. Furthermore, other functions are demonstrated for the snoRNAs such as the implication in post-transcriptional or in directing alternative splicing regarding specific mRNAs coding for proteins (Makarova et al., 2013). These short RNA molecules can be also the precursors of other small regulative RNAs like miRNAs and sno-derived RNAs (**sdRNAs**). All these findings are quite recent and validated only in few experiments. If these regulatory mechanisms can be confirmed, a specific role in regulating the muscle development could be found.

The second group of noncoding regulated transcripts includes 5 miRNAs that have been precisely

Table 7. Identification of the type of the regulated small nucleolar RNAs.

Name GG	GB GG	nt GG	Name HS	GB HS	nt HS	Coverage (%)	Identity (%)	Full name
GGN5	EU240224	135	SNORA55	NR_002983	137	99	81	small nucleolar RNA, H/ACA box 55
GGN50	EU240266	132	SNORA22	NR_002961	134	99	82	small nucleolar RNA, H/ACA box 22
GGN73	EU240289	137	SNORA46	NR_002978	135	57	84	small nucleolar RNA, H/ACA box 46
GGN98	EU240313	129	SNORA28	NR_002964	126	38	84	small nucleolar RNA, H/ACA box 28

GG = *Gallus gallus*; HS = *Homo sapiens*.

Table 8. Predicted overexpressed target genes found in miRBase for the differentially expressed miRNAs.

gga-miR-196-5p	gga-miR-205a	gga-miR-1600	gga-miR-1716	gga-miR-1805-3p
FAM64A	*LOC425021* *NMT2* *PLXNA1*	*ANKRD31* *PLN* *PRRX2*	–	*WDFY3*

identified by searching on miRBase. Furthermore, on the same database we searched for the putative target genes using as entry the DE chicken miRNAs and the overexpressed coding genes, according to miRNA repressive mechanism of regulation, as indication of a direct regulation (Table 8). 4 out of 5 miRNAs have been indicated as putative regulators of 8 genes: ankyrin repeat domain 31 (***ANKRD31***); family with sequence similarity 64, member A (***FAM64A***); PQ-loop repeat-containing protein 2-like (***LOC425021***); N-myristoyltransferase 2 (***NMT2***); phospholamban (***PLN***); plexin A1 (***PLXNA1***); paired-related homeobox 2 (***PRRX2***); and WD repeat and FYVE domain containing 3 (***WDFY3***).

DISCUSSION

WS and WB are abnormalities of chicken breast skeletal muscle observed quite frequently in most of modern broiler hybrids (Petracci et al., 2015). In the present study, the gene expression and the meat quality traits of affected chickens' pectoralis major muscles were investigated, in order to evaluate the effects exerted by these pathologic conditions on the gene transcription levels and the fillets' biochemical composition. On the whole, the results outlined the presence of a severely damaged pectoralis major muscle, with ABN samples showing consistent changes in the expression level of genes related to muscle development, reactive oxygen species metabolism, oxidative stress and signal transduction, blood vessel morphogenesis, and polysaccharide metabolism. Considering the data reported in the present study, together with the results identified in literature (Kuttappan et al., 2013; Sihvo et al., 2014, Mazzoni et al., 2015; Mutryn et al., 2015; Soglia et al., 2016), a consistent impairment of normal muscle metabolism is evident for WS/WB defects and these abnormalities appear to be linked to a complex pathogenesis.

To date, the complex pathological framework characterizing WS/WB defects has made it extremely difficult to identify the underlying causes at the basis of the alterations. Despite agreement in the literature about WS and WB defects regarding the large number of histological, biochemical and metabolic alterations accompanying the occurrence of these breast muscle abnormalities, there is no consensus on the causes leading to the insurgence of this complex pathological framework. The results obtained from the present research have been evaluated and discussed in the light of the knowledge reported to date in literature on WS and WB topics, aiming to outline an overall view of the pathological changes affecting pectoralis major muscle showing in addition the gene networks and the biological evidences related to the occurrence of the WS/WB tissue alterations. Furthermore, the overall analysis of the variations obtained to date at the genetic, biochemical, biological, and histological levels allows defining some possible hypotheses on the mechanisms determining the onset of these myopathies.

Oxidative Stress

In the present research, the microarray data showed an overall increase in the expression level of genes involved in the response against the accumulation of hydrogen peroxide and reactive oxygen species in ABN fillets, in agreement with the presence of an oxidative stress possibly linked to a muscle hypoxic condition. In particular, ABN samples presented increased expression levels of crystallin alpha B (***CRYAB***), adenosine deaminase (***ADA***), *MB* genes and a decreased activity of reactive oxygen species modulator 1 (***ROMO1***) gene, that are all involved in the response to reactive oxygen species (Table 6 and Supplementary Table 2). These results agree with Mutryn et al. (2015) that identified a set of DE genes involved in myofibers reaction to oxidative stress in muscle samples of high breast yield chickens affected by WS/WB. The cause of this oxidative stress is not clear, although past studies can help defining some possible causes. One of the possible hypotheses reported in literature indicates an inadequate breast muscle vascularizsation as a possible key factor in WS/WB occurrence (Mutryn et al., 2015). It

is worth to note that in 1999, Dransfield and Sosnicki reported an increased proportion of glycolytic fibers with enlarged diameter in chicken lines selected for high growth rate and breast yield (Dransfield and Sosnicki, 1999). Moreover, Hoving-Bolink et al. (2000) showed an intense reduction in both vascularization and capillary to fiber ratio in chicken hybrids selected for high growth rate and breast yield compared to unselected chicken lines. Based on these results genetic selection in these chicken lines determined in muscles an inadequate blood vessel growth with the consequent impairment in oxygen supply and in the metabolic waste products displacement from breast myofibers. In agreement with Mutryn et al. (2015), also the present results indicated that an excessive accumulation of reactive oxygen species (**ROS**) within the muscle tissue of ABN samples might be involved in initiating the inflammatory mechanism typically associated with WS and/or WB muscle abnormalities.

Inflammation and Myofiber Degeneration

The profound alterations and the inflammatory status observed in previous researches were confirmed in the present study where an increased transcription of genes coding for proteins involved in biological processes related to tissue alteration was detected. More precisely, we have found that immunoglobulin superfamily, member 10 gene (***IGSF10***), heat shock 105 kDa/110 kDa protein 1 (***HSPH1***) and heat shock 60 kDa protein 1 (Chaperonin) (***HSPD1***) were overexpressed in ABN samples (Supplementary Table 2), supporting the presence of the tissue inflammation. Moreover, the overexpression in ABNs of ADAM family metallopeptidase with thrombospondin type 1 motif 12 (***ADAMTS12***) and ADAM metallopeptidase with thrombospondin type 1 motif 19 (***ADAMTS19***; Supplementary Table 2) genes suggested the existence of a muscle tissue inflammation, as *ADAMTS12* in particular is already known to be involved in the activation of inflammatory responses (Moncada-Pazos et al., 2012). Similarly, the higher transcription levels of nuclear factor, interleukin 3 regulated (***NFIL3***) and snail family zinc finger 2 (***SNAI2***; Supplementary Table 2), as genes encoding for hindering-cell death molecules (Keniry et al., 2014), could reveal the attempt to limit apoptotic processes and necrosis of the cells. Thus, the onset of a complex biological reaction aimed at contrasting the inflammatory process with the activation of anti-inflammatory responses was observed in ABN samples. These inflammatory and necrotic processes were previously found in WS and WB breast muscles (Kuttappan et al., 2013; Sihvo et al., 2014; Mutryn et al., 2015) and association to degenerative processes of muscular nerve growth was hypothesized. Indeed, the microarray analysis evidenced in WS/WB broilers reduced transcription levels of the genes deafness autosomal recessive 31 (***DFNB31***), syntaxin 3 (***STX3***), neurogenin 1 (***NEUROG1***), SLIT and NTRK-like family member 6 (***SLITRK6***), wingless-type MMTV integration site family member 7A (***WNT7A***), and EPH receptor A2 (***EPHA2***), involved in neuron genesis and differentiation as indicated by DAVID analysis.

Another differentially expressed gene found in the present study is interleukin 1 beta (***IL1B***), which encodes for a member of the interleukin 1 cytokine family. This protein exerts a central role as mediator of the inflammatory response and is involved in a variety of cellular activities (including cell proliferation, differentiation and apoptosis). Although the findings of the present study outlined an inflammatory process affecting ABN samples, a down-regulated transcription of *IL1B* gene was found (Supplementary Table 2). Despite the majority of the literature reports in muscles affected by inflammation an increased expression level of the *IL1B* gene (Dinarello, 1998; Li et al., 2008), in some cases this gene was found down-regulated during some chronic pathological situations (Karli et al., 2014). Moreover it is possible to hypothesize that the reduced transcription level of *IL1B* identified within the WS/WB samples could be linked to the low level of vascularization of the ABN samples as IL1B was also found to play a relevant role in the angiogenic processes promoting the emergence of new capillaries from pre-existing blood vessels (Dinarello, 1996; Voronov et al., 2003). Furthermore, as interleukin 1 has a pyrogenic role and its involvement in the pain sensation during inflammation has been evidenced, the down-regulation of *IL1B* transcription might be responsible for the lack of symptoms in chickens affected by WB/WS abnormalities during the broiler farming period.

Some genes identified as differentially expressed have been reported in literature to be associated with the development of myopathies. The over-expression of *PLN* observed in ABN samples (Supplementary Table 2) was related in mice muscles to an altered phenotype similar to the centronuclear myopathy identified in human muscles (Fajardo et al., 2015). Centronuclear myopathy is a congenital myopathy characterized by centrally located nuclei, a peculiarity that was already described in WS/WB affected muscles (Sihvo et al., 2014; Soglia et al., 2016).

Moreover, *ATP2A2* gene and protein was found overexpressed in ABN samples. Soglia et al. (2016) reported that an impaired activity of AT2A2 protein might be involved in the WS/WB phenotype with a loss of adhesion among myocytes and the presence of abundant connective tissue replacing the muscle cells. This phenomenon is for some instances similar to a human pathology, Darier-White disease (Savignac et al., 2011), which is characterized by a loss of adhesion between epidermal cells and keratinization leading to apoptosis of the same cells. The causative mutation of the human disease was found in one of the transcripts of *ATP2A2* gene.

Myofibers Regeneration

In the present study, several genes involved in muscle development and cell differentiation were found differentially expressed within the ABN cases (Table 7). In particular, the over-expression of *CSRP3* and *PTGFR* as well as the down-regulation of *P2RY1* gene identified in the present research, could be associated respectively to muscle fibers synthesis (Kong et al., 1997; Jansen and Pavlath, 2008) and myogenesis (Krasowska et al., 2014).

The cascade pathway of *PTGFR*, *PLN*, *GNAQ*, *PLCB2*, and *PLCD1* has been also related to mechanisms aimed at regenerating damaged muscle. The combined activity of these 5 DEG triggers several downstream metabolic pathways that increase muscle cells volume (Horsley and Pavlath, 2003, 2004; Hindi et al., 2013) and contribute to the regeneration of myofibers upon injury, suggesting a possible role of these genes in trying to repair the effect of severe pectoralis major myopathies such as WB and WS.

Additionally, ABN fillets showed an increased mRNA level of the gene *FAM64A*. The expression of this gene was reported to be associated with rapidly proliferating tissues during mouse embryogenesis (Archangelo et al., 2008). Based on this previous finding, *FAM64A* overexpression may be associated to the regeneration processes taking place in the damaged breasts, and its up-regulation could be determined by gga-miR-196-5p that identifies *FAM64A* as a specific target gene (Table 8). Similarly, also increased mRNA levels of *PLXNA1* and *PRRX2* genes, up-regulated in ABN samples, have been related to proliferating fetal fibroblasts and developing tissue (White et al., 2003; Hota and Buck, 2012). As suggested for *FAM64A,* we hypothesize that *PLXNA1* and *PRRX2* expression changes may be respectively linked to the regulation exerted by gga-miR-205a and gga-miR-1600. Anyway, these hypotheses will need further studies to be proven.

On the whole, the results obtained from the microarray, with DE genes from pathways linked to muscle differentiation and development, can be interpreted as the evidences of an activation of muscle cells regenerative processes in response to the degenerative status. These tissue regenerative processes (nuclear rowing and cell multi-nucleation) have been evidenced within the WS/WB muscles in previous histological observations (Kuttappan et al., 2013; Sihvo et al., 2014, Soglia et al., 2016). Furthermore, a remarkable increase in the amount of AT2A2 (Table 5) coupled with an over-expression of *ATP2A2* gene and *MB* gene, was detected in ABN samples similar to what was observed by Mutryn et al. (2015) in muscles affected by WB abnormality. These Authors supposed that the higher expression of *ATP2A2* and *MB* might be the result of a shift from type IIb towards slow twitch type I fibers in abnormal breast muscles. This reorganization of the tissue might be explained considering that similar regenerative mechanisms, exhibiting an overall increase in slow-twitch fibers and the apoptosis of the fast-twitch ones, were previously observed in mice dystrophic muscles (Massa et al., 1997). In addition, the up-regulation in the transcription of acetyl-CoA acyltransferase 2 (***ACAA2***) gene, encoding for a protein exerting a relevant role in the metabolic pathway leading to mitochondrial beta oxidation of fatty acids, might support the hypothesized shift of ABN muscles towards oxidative metabolism.

Impaired Muscle Ion Homeostasis

ABN samples showed relevant changes in their chemical composition, with an overall modification in mineral content (Table 3). In particular, the increased sodium content may be related to the more elevated transcription of solute carrier family 9, subfamily A (NHE7, cation proton antiporter 7) member 7 (***SLC9A7***) gene, as it encodes a sodium and potassium/ proton antiporter (Kagami et al., 2008).

Additionally, also increased levels of calcium were identified in ABN samples (Table 3), supporting the existence of the intracellular calcium buildup already hypothesized by Mutryn et al. (2015) on the basis of the altered transcription levels identified for genes involved in calcium homeostasis. In agreement with this hypothesis, several genes linked to intracellular ion homeostasis were found differentially expressed in the present study (Figure 2), in particular the up-regulation of genes linked to the activation of G protein–coupled purinergic receptors was observed in cascade in ABN samples. The over-expression of *PTGFR* coupled with the increase in guanine nucleotide binding protein (G protein) alpha 11 (***GNAQ***) and G protein-coupled receptor 1 (***GPR1***) might be related to the up-regulation of phospholipase C beta 2 (***PLCB2***) and phospholipase C delta 1 (***PLCD1***) genes (Figure 3), involved in the processes leading to the increase of Ca^{2+} in the cells. According to Bucheimer and Linden (2004), the G protein–coupled receptors activate β phospholipase enzymes, resulting in an increased intracellular Ca^{2+} concentration and altered ions homeostasis. Within this framework, the reduced expression of calcium homeostasis modulator 3 gene (***CALHM3***; Supplementary Table 2), the higher synthesis of AT2A2 protein and the increased transcription of its relative gene *ATP2A2* and *PLN* gene can produce in ABN samples an overall alteration in calcium signaling pathway, contributing to the inflammatory processes. *ATP2A2* over-expression was noticed also by Mutryn et al. (2015) in breast muscles affected by WB abnormality.

Between the differentially expressed miRNAs, gga-miR-1600 may be the putative regulator of *PLN* gene expression (Table 8), suggesting that for calcium signaling pathway a higher level of regulation might be responsible of relevant changes in the molecular mechanisms involved in the origin of the WB/WS myopathy.

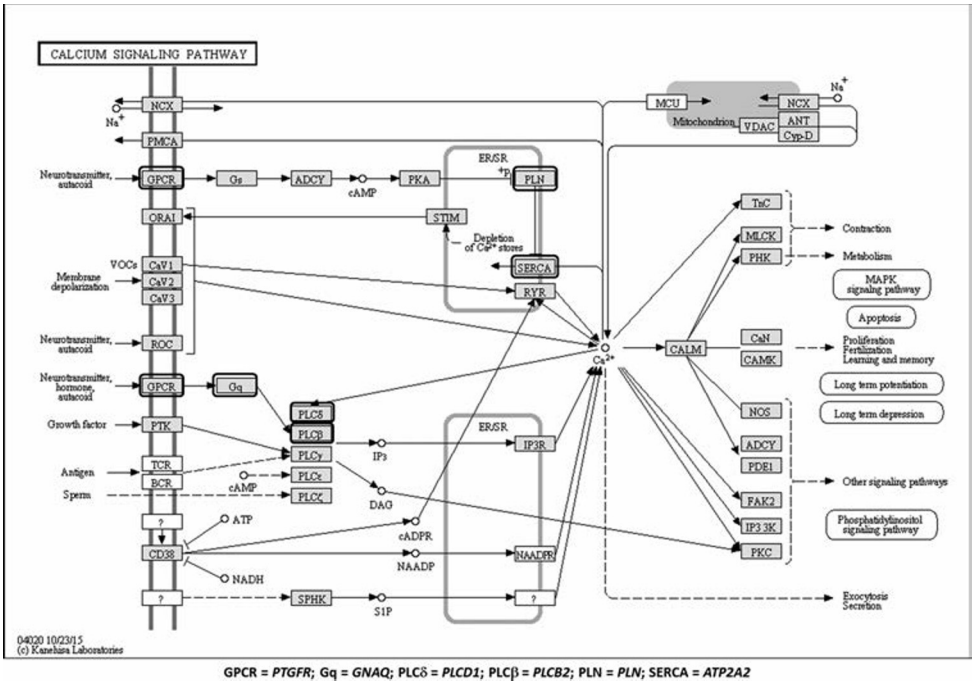

Figure 2. KEGG table representing the calcium signaling pathway. The differentially expressed genes found are indicated with black circles.

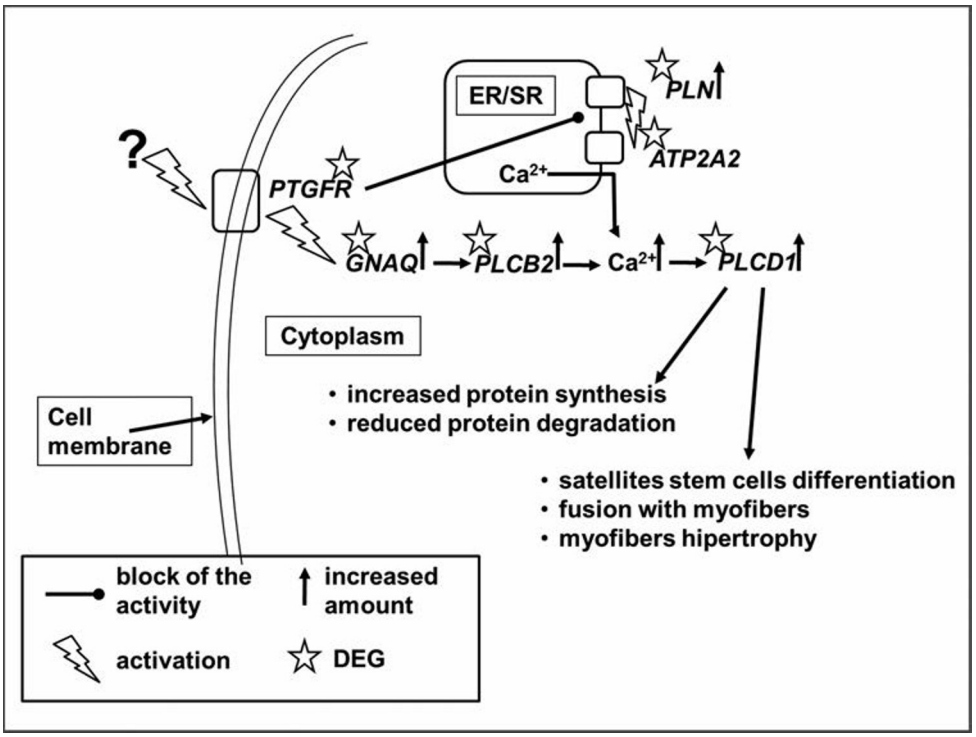

Figure 3. A putative mechanism explaining some of the changes occurring in abnormal muscle samples deduced from the activities of the differentially expressed genes involved in calcium signaling pathway.

Anyway, on the basis of the whole literature produced to date, it is not possible to formulate a certain assumption about the causes leading to this overall impairment in muscle ion homeostasis. The differential expression of genes related to the purinergic receptors pathways that we found in ABN samples may be one of the primary causes of the inflammation or, most likely, one of the effects of muscle tissue structural changes related to WS/WB abnormalities and the results of the activation of the purinergic receptors from the ATP released in the extracellular matrix spaces from damaged fibers (Bucheimer and Linden, 2004; Eltzschig et al., 2012).

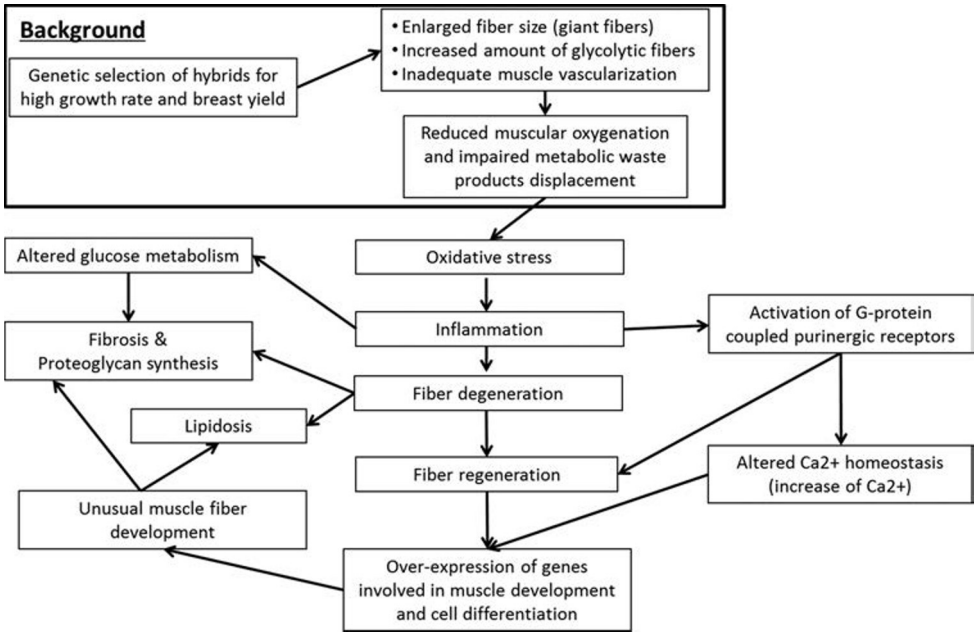

Figure 4. A schematic representation of one of the possible etiologies at the basis of white striping and wooden breast abnormalities.

Altered Glucose Metabolism, Lipidosis, Fibrosis, and Proteoglycan Synthesis

The SDS-PAGE results revealed an intensified glycolytic activity in ABN samples, with higher amount of glycolytic enzymes such as lactate dehydrogenase (**LDH**), glyceraldehyde dehydrogenase (**G3P**), aldolase (**ALDO**) and glycogen phosphorylase (**PYGL**). Among the glycolytic enzymes, the magnesium-dependent enzymes phosphoglycerate mutase (**PGAM**), phosphoglucose isomerase (**GPI**) and pyruvate kinase (**KPYM**) were less expressed in ABN samples. The inadequate level of disposable magnesium in affected muscles (Table 3) could be linked to the lower translation of these magnesium-dependent enzymes in affected samples. A general modification of the glycolytic enzymes expression was evident in ABN pectoralis major muscles. Despite the increased synthesis of LDH enzyme in ABN samples, a higher ultimate pH in the affected breast muscles was observed (Table 2), suggesting that there was not an increase in the transformation of pyruvate into lactate, as normally expected in hypoxic conditions. In addition to the modifications in glycolytic enzymes synthesis, we found by microarray analysis that in ABN samples the genes *GNE*, glycogen branching enzyme (***GBE1***), UDP-glucose 6-dehydrogenase (***UGDH***), and protein phosphatase 1, catalytic subunit, beta isozyme (***PPP1CB***), involved in polysaccharide metabolic processes were overexpressed (Supplementary Table 2). GNE enzyme plays an essential role in hexosamine pathway, in particular for the biosynthesis of N-acetylneuraminic acid, a precursor of sialic acids. This evidence might suggest an alternative utilization of fructose 6-phosphate, produced by PGI enzyme during glycolysis. Indeed fructose 6-phosphate can undertake the glycolysis pathway or can be used as the initial substrate of the hexosamine and hexuronic acid pathways, resulting in collagen, proteoglycans and glycosaminoglycans synthesis. This shift towards hexosamine pathway was also described by Du et al. (2000) as a consequence of the accumulation of ROS species, which otherwise exerted an inhibitory effect on glycolysis. On the other hand, UGDH converts UDP-glucose to UDP-glucuronate and thereby participates in the biosynthesis of glycosaminoglycans such as hyaluronan (a common component of the extracellular matrix). The over-expressions of *UGDH, GNE*, *GBE1*, *PPP1CB* and interphotoreceptor matrix proteoglycan 2 (***IMPG2***) genes identified in the present research, together with the observed fibrosis described on the same samples by Soglia et al. (2016), could explain the increased presence of collagen and proteoglycans in the areas affected by WS/WB lesions. These findings agree with the evidences reported in literature for WS and/or WB abnormalities (Kuttappan et al., 2013; Sihvo et al., 2014; Mutryn et al., 2015; Velleman and Clark, 2015).

Additionally, the increased collagen and fat contents observed in ABN samples (Table 3) were in agreement with previous findings (Kuttappan et al., 2013; Mudalal et al., 2014; Soglia et al., 2016). A similar situation was described by Lopes-Ferreira et al. (2001), who noticed in hypoxic conditions the development of both fibrosis and lipidosis within the skeletal muscle, with a replacement of the lost fibers with the collagen synthesis and lipid deposition.

The present results, combined with the existing knowledge, allowed to draw a scheme (Figure 4) describing a possible progression of the biological processes cascade hypothesized to be involved in the development of WS/WB myopathies.

On the whole, the findings of the present study show at the gene level that a complex etiology is associated

with the occurrence of WS and WB muscle abnormalities. In WS/WB breast muscles, there is evidence of differentially expressed genes related to several functional categories: muscle development, polysaccharide metabolic processes, glucose metabolism, proteoglycans synthesis, inflammation, and calcium signaling pathway. By combining the functional roles for the differentially expressed genes, we hypothesized a network of biological changes that are acting simultaneously and are responsible for the phenotypic evidences of these myopathies.

Although the cause of these myopathies is still unclear, the majority of the results reported in literature suggests that selection criteria more and more addressed towards fast growing and high breast yield broilers could be involved in the occurrence of the breast oxidative stress that triggers the cascade of WS/WB related muscle alterations. The data obtained in the present research can be useful for the clarification of the WS/WB pathogenesis and further studies have to be planned to disentangle the complex etiology behind these myopathies.

SUPPLEMENTARY DATA

Supplementary data are available at *PSCIEN* online.

Supplementary Table 1. Primers and PCR conditions used for the validation performed using qPCR.

Supplementary Table 2. List of the differentially expressed genes obtained by microarray analysis.

REFERENCES

Alnahhas, N., C. Berri, M. Chabault, P. Chartrin, M. Boulay, M. C. Bourin, and E. Le Bihan-Duval. 2016. Genetic parameters of white striping in relation to body weight, carcass composition, and meat quality traits in 2 broiler lines divergently selected for the ultimate pH of the pectoralis major muscle. BMC Genet. 17:61.

AOAC. 1990. Meat and meat products. Pages 931–948 in Official Methods of Analysis. 15th ed. Vol. 2. Assoc. Off. Anal. Chem., Washington, DC.

Archangelo, L. F., P. A. Greif, M. Hölzel, T. Harasim, E. Kremmer, G. K. H. Przemeck, D. Eick, A. J. Deshpande, C. Buske, M. Hrabé de Angelis, S. T. Olalla Saad, and S. K. Bohlander. 2008. The CALM and CALM/AF10 interactor CATS is a marker for proliferation. Mol. Oncol. 2:356–367.

Bailey, R. A., K. A. Watson, S. F. Bilgili, and S. Avendano. 2015. The genetic basis of pectoralis major myopathies in modern broiler chicken lines. Poult. Sci. 94:2870–2879.

Bradford, M. M. 1976. A rapid and sensitive method for the quantitation of microgram quantities of protein utilizing the principle of protein-dye binding. Anal Biochem. 72:248–254.

Bucheimer, R. E., and J. Linden. 2004. Purinergic regulation of epithelial transport. J. Physiol. 555:311–321.

Davoli, R., S. Braglia, V. Russo, L. Varona, and M. F. W. te Pas. 2011. Expression profiling of functional genes in prenatal skeletal muscle tissue in Duroc and Pietrain pigs. J. Anim. Breed. Genet. 128:15–27.

Dinarello, C. A. 1996. Biologic basis for interleukin-1 in disease. Blood. 87:2095–2147.

Dinarello, C. A. 1998. Interleukin-1, interleukin-1 receptors and interleukin-1 receptor antagonist. Int. Rev. Immunol. 16:457–499.

Dransfield, E., and A. A. Sosnicki. 1999. Relationship between muscle growth and poultry meat quality. Poult. Sci. 78:743–746.

Du, X. L., D. Edelstein, L. Rossetti, I. G. Fantus, H. Goldberg, F. Ziyadeh, J. Wu, and M. Brownlee. 2000. Hyperglycemia-induced mitochondrial superoxide overproduction activates the hexosamine pathway and induces plasminogen activator inhibitor-1 expression by increasing Sp1 glycosylation. Proc. Natl. Acad. Sci. U.S.A. 97:12222–12226.

Eltzschig, H. K., M. V. Sitkovsky, and S. C. Robson. 2012. Purinergic signaling during inflammation. N. Engl. J. Med. 367:2322–2333.

Environmental Protection Agency, Office of Solid Waste. 1996. Method 3052. Microwave Assisted Acid Digestion Of Siliceous And Organically Based Matrices. U.S. EPA, Washington, DC. http://www.epa.gov/osw/hazard/testmethods/sw8467pdfs/3052.pdf.

Environmental Protection Agency, Office of Solid Waste. 2007. Method 6010C. Inductively Coupled Plasma-Atomic Emission Spectrometry.U.S. EPA, Washington, DC. http://www.epa.gov/osw/hazard/testmethods/sw846/pdfs/6010c.pdf.

Fajardo, V. A., E. Bombardier, E. McMillan, K. Tran, B. J. Wadsworth, D. Gamu, A. Hopf, C. Vigna, I. C. Smith, C. Bellissimo, R. N. Michel, M. A. Tarnopolsky, J. Quadrilatero, and A. R. Tupling. 2015. Phospholamban overexpression in mice causes a centronuclear myopathy-like phenotype. Dis. Model Mech. 8:999–1009.

Hindi, S. M., M. M. Tajrishi, and A. Kumar. 2013. Signaling mechanisms in mammalian myoblast fusion. Sci. Signal. 6:re2–re2.

Holley, C. L., and V. K. Topkara. 2011. An introduction to small non-coding RNAs: miRNA and snoRNA. Cardiovasc. Drugs Ther. 25:151–159.

Horsley, V., and G. K. Pavlath. 2003. Prostaglandin F2 (alpha) stimulates growth of skeletal muscle cells via an NFATC2-dependent pathway. J. Cell Biol. 161:111–118.

Horsley, V., and G. K. Pavlath. 2004. Forming a multinucleated cell: molecules that regulate myoblast fusion. Cells Tissues Organs. 176:67–78.

Hota, P. K., and M. Buck. 2012. Plexin structures are coming: opportunities for multilevel investigations of semaphorin guidance receptors, their cell signaling mechanisms, and functions. Cell Mol. Life Sci. 69:3765–3805.

Hoving-Bolink, A. H., R. W. Kranen, R. E. Klont, C. L. M. Gerritsen, and K. H. de Greef. 2000. Fiber area and capillary supply in broiler breast muscle in relation to productivity and ascites. Meat Sci. 56:397–402.

Huang, D. W., B. T. Sherman, and R. A. Lempicki. 2009a. Systematic and integrative analysis of large gene lists using DAVID bioinformatics resources. Nat. Protoc. 4:44–57.

Huang, D. W., B. T. Sherman, and R. A. Lempicki. 2009b. Bioinformatics enrichment tools: paths toward the comprehensive functional analysis of large gene lists. Nucleic Acids Res. 37:1–13.

Jansen, K. M., and G. K. Pavlath. 2008. Prostaglandin F2α promotes muscle cell survival and growth through upregulation of the inhibitor of apoptosis protein BRUCE. Cell Death Differ. 15:1619–1628.

Jeacocke, R. E. 1977. The temperature dependence of anaerobic glycolysis in beef muscle held in a linear temperature gradient. J. Sci. Food Agric. 28:551–556.

Kagami, T., S. Chen, P. Memar, M. Choi, L. J. Foster, and M. Numata. 2008. Identification and biochemical characterization of the SLC9A7 interactome. Mol. Membr. Biol. 25:436–447.

Karli, P., V. Martlé, K. Bossens, A. Summerfield, M. G. Doherr, P. Turner, M. Vandevelde, F. Forterre, and D. Henke. 2014. Dominance of chemokine ligand 2 and matrix metalloproteinase-2 and -9 and suppression of pro-inflammatory cytokines in the epidural compartment after intervertebral disc extrusion in a canine model. Spine J. 14:2976–2984.

Keniry, M., R. K. Dearth, M. Persans, and R. Parsons. 2014. New Frontiers for the NFIL3 bZIP Transcription Factor in Cancer, Metabolism and Beyond. Discoveries. 2:e15.

Kolar, K. 1990. Colorimetric determination of hydroxyproline as measure of collagen content in meat and meat products: NMKL collaborative study. J. Assoc. Off. Anal. Chem. 73:54–57.

Kong, Y., M. J. Flick, A. J. Kudla, and S. F. Konieczny. 1997. Muscle LIM protein promotes myogenesis by enhancing the activity of MyoD. Cell. Mol. Biol. 17:4750–4760.

Krasowska, E., J. Róg, A. Sinadinos, C. N. J. Young, D. C. Górecki, and K. Zabłocki. 2014. Purinergic receptors in skeletal muscles in health and in muscular dystrophy. Postepy. Biochem. 60:483–489.

Kuttappan, V. A., Y. S. Lee, G. F. Erf, J. F. Meullenet, S. R. McKee, and C. M. Owens. 2012. Consumer acceptance of visual appearance of broiler breast meat with varying degrees of white striping. Poult. Sci. 91:1240–1247.

Kuttappan, V. A., H. L. Shivaprasad, D. P. Shaw, B. A. Valentine, B. M. Hargis, F. D. Clark, S. R. McKee, and C. M. Owens. 2013. Pathological changes associated with white striping in broiler breast muscles. Poult. Sci. 92:331–338.

Li, L., Z. Fei, J. Ren, R. Sun, Z. Liu, Z. Sheng, L. Wang, X. Sun, J. Yu, Z. Wang, and J. Fei. 2008. Functional imaging of interleukin 1 beta expression in inflammatory process using bioluminescence imaging in transgenic mice. BMC Immunol. 9:49.

Li, K., Y. Y. Zhao, Z. L. Kang, P. Wanh, M. Y. Han, X. L. Xu, and G. H. Zhou. 2015 Reduced functionality of PSE-like chicken breast meat batter resulting from alterations in protein conformation. Poult. Sci. 94:111–122.

Liu, J., M. Ruusunen, E. Puolanne, and P. Ertbjerg. 2014. Effect of pre-rigor temperature incubation on sarcoplasmic protein solubility, calpain activity and meat properties in porcine muscle. LWT Food Sci. Technol. 55:483–489.

Lopes-Ferreira, M., J. Núñez, A. Rucavado, S. H. Farsky, B. Lomonte, Y. Angulo, A. M. Moura Da Silva, and J. M. Gutiérrez. 2001. Skeletal muscle necrosis and regeneration after injection of *Thalassophryne nattereri* (niquim) fish venom in mice. Int. J. Exp. Pathol. 82:55–64.

Lorenzi, M., S. Mudalal, C. Cavani, and M. Petracci. 2014. Incidence of white striping under commercial conditions in medium and heavy broiler chickens in Italy. J Appl. Poult. Res. 23:754–758.

Makarova, J. A., S. M. Ivanova, A. G. Tonevitsky, and A. I. Grigoriev. 2013. New functions of small nucleolar RNAs. Biochemistry (Mosc.) 78:638–650.

Massa, R., G. Silvestri, Y. C. Zeng, A. Martorana, G. Sancesario, and G. Bernardi. 1997. Muscle regeneration in mdx mice: resistance to repeated necrosis is compatible with myofiber maturity. Basic Appl. Myol. 7:387–394.

Mazzoni, M., M. Petracci, A. Meluzzi, C. Cavani, P. Clavenzani, and F. Sirri. 2015. Relationship between pectoralis major muscle histology and quality traits of chicken meat. Poult. Sci. 94:123–130.

Moncada-Pazos, A., A. J. Obaya, M. Llamazares, R. Heljasvaara, M. F. Suárez, E. Colado, A. Noël, S. Cal, and C. López-Otín. 2012. ADAMTS-12 metalloprotease is necessary for normal inflammatory response. J. Biol. Chem. 287:39554–39563.

Mudalal, S., E. Babini, C. Cavani, and M. Petracci. 2014. Quantity and functionality of protein fractions in chicken breast fillets affected by white striping. Poult. Sci. 93:2108–2116.

Mudalal, S., M. Lorenzi, F. Soglia, C. Cavani, and M. Petracci. 2015. Implications of white striping and wooden breast abnormalities on quality traits of raw and marinated chicken meat. Animal. 9:728–734.

Mutryn, M. F., E. M. Brannick, W. Fu, W. R. Lee, and B. Abasht. 2015. Characterization of a novel chicken muscle disorder through differential gene expression and pathway analysis using RNA-sequencing. BMC Genomics. 16:399.

Petracci, M., and C. Cavani. 2012. Muscle growth and poultry meat quality issues. Nutrients. 4:1–12.

Petracci, M., S. Mudalal, A. Bonfiglio, and C. Cavani. 2013. Occurrence of white striping under commercial conditions and its impact on breast meat quality in broiler chickens. Poult. Sci. 92:1670–1675.

Petracci, M., S. Mudalal, F. Soglia, and C. Cavani. 2015. Meat quality in fast-growing broiler chickens. Worlds Poult. Sci. J. 71:363–374.

Pfaffl, M. W. 2004. Quantification strategies in real-time PCR. Pages 87–112 in A–Z of Quantitative PCR, S. A. Bustin, ed. International University Line, La Jolla, CA.

Sandercock, D. A., Z. Barker, M. A. Mitchell, and P. H. Hocking. 2009. Changes in muscle cell cation regulation and meat quality traits are associated with genetic selection for high body weight and meat yield in broiler chickens. Genet. Sel. Evol. 41:8.

Savignac, M., A. Edir, M. Simon, and A. Hovnanian. 2011. Darier disease: a disease model of impaired calcium homeostasis in the skin. Biochim. Biophys. Acta. 1813:1111–1117.

Sihvo, H. K., K. Immonen, and E. Puolanne. 2014. Myodegeneration with fibrosis and regeneration in the pectoralis major muscle of broilers. Vet. Pathol. 51:619–623.

Soglia, F., S. Mudalal, E. Babini, M. Di Nunzio, M. Mazzoni, F. Sirri, C. Cavani, and M. Petracci. 2016. Histology, composition, and quality traits of chicken Pectoralis major muscle affected by wooden breast abnormality. Poult. Sci. 95:651–659.

Velleman, S. G., and D. L. Clark. 2015. Histopathologic and Myogenic Gene Expression Changes Associated with Wooden Breast in Broiler Breast Muscles. Avian Dis. 59:410–418.

Voronov, E., D. S. Shouval, Y. Krelin, E. Cagnano, D. Benharroch, Y. Iwakura, C. A. Dinarello, and R. N. Apte. 2003. IL-1 is required for tumor invasiveness and angiogenesis. Proc. Natl Acad. Sci. U.S.A. 100:2645–2650.

White, P., D. W. Thomas, S. Fong, E. Stelnicki, F. Meijlink, C. Largman, and P. Stephens. 2003. Deletion of the homeobox gene PRX-2 affects fetal but not adult fibroblast wound healing responses. J. Invest. Dermatol. 120:135–144.

Zambonelli, P., E. Gaffo, M. Zappaterra, S. Bortoluzzi, and R. Davoli. 2016. Transcriptional profiling of subcutaneous adipose tissue in Italian Large White pigs divergent for backfat thickness. Anim. Genet. 47:306–323.

Zapata, I., J. M. Reddish, M. A. Miller, M. S. Lilburn, and M. Wick. 2012. Comparative proteomic characterization of the sarcoplasmic proteins in the pectoralis major and supracoracoideus breast muscles in 2 chicken genotypes. Poult. Sci. 91:1654–1659.

Zhang, Y., J. Wang, S. Huang, X. Zhu, J. Liu, N. Yang, D. Song, R. Wu, W. Deng, G. Skogerbø, X.-J. Wang, R. Chen, and D. Zhu. 2009. Systematic identification and characterization of chicken (*Gallus gallus*) ncRNAs. Nucleic Acids Res. 37:6562–6574.